

DEPTH-AVERAGED FLOW FIELDS IN MEANDERING CHANNELS WITH ALLUVIAL EQUILIBRIUM BED

Nobuyuki Tamai, Professor
Ali A. Mohamed, Graduate Student
University of Tokyo

1. INTRODUCTION

A characteristic feature of the mechanics of alluvial channels is that the bed is self-formed by the interaction of flow and sediment motion. In this paper a mathematical analysis of the longitudinal variation of the depth-averaged flow in continuous river bends with alluvial equilibrium bed is developed. A new expression for the bed topography is applied apart from an exponential function utilized by Engelund (1). The solution is obtained up to the second order in terms of ε by a perturbation method. The results are compared with existing experimental data.

2. THEORY

2.1 Coordinate System and Governing Equations

The theoretical solution is derived for meandering channels the centerline of which coincide with the sine-generated curve.

$$\theta = \theta_0 \sin \frac{2\pi s_c}{L} \quad (1)$$

where θ = the angle between the tangent of the channel centerline and the down-valley direction at a distance s_c from the origin measured along the channel centerline, θ_0 = the maximum angle between the centerline and the valley axis, L = the meandering length of one meander along the centerline and s_c = the distance along the centerline of the channel (see Fig. 1).

In this theory, it is utilized the three dimensional coordinate system (s, n, z) in which (s, n) composes an orthogonal curvilinear coordinate system (3). The n -coordinate is the transverse distance measured from the centerline and perpendicular to s on the same plane of s . The origin of s -coordinate is the location where $\theta = 0$. z is the vertical coordinate taken positive upward.

The main assumptions in the governing equations utilized in this theory are explained in previous paper (3). In this paper, it is assumed that the longitudinal component of the bed shear stress is sufficiently close to the total bed shear.

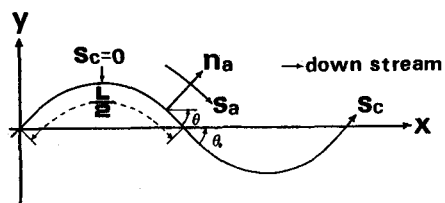


Fig. 1 Coordinate system

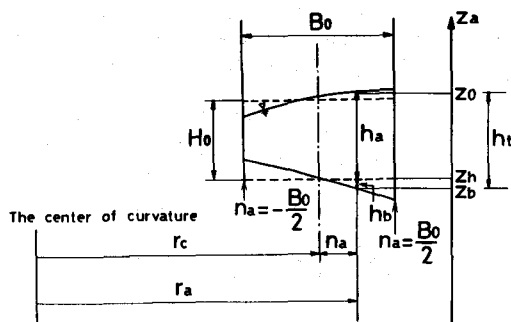


Fig. 2 Cross section of the channel and symbols

$$\frac{\tau_o}{\rho} = \frac{1}{2} f (u_s)^2 \quad (2)$$

where f is the friction coefficient.

For convenience let us begin with the nondimensional form of the governing equations (3).

$$\varepsilon \frac{\partial}{\partial s} [(h + \eta) u] + \frac{\partial}{\partial n} \left[\frac{r_a}{r_c} (h + \eta) v \right] = 0 \quad (3)$$

$$\frac{1}{2} \int_{-1}^1 (h + \eta) u \, dn = 1 \quad (4)$$

$$u \frac{\partial u}{\partial s} + \frac{r_a}{r_c} \frac{1}{\varepsilon} v \frac{\partial u}{\partial n} + \frac{R}{r_c} uv = \frac{1}{F_r^2} \frac{\partial h}{\partial s} + \frac{gIR}{V^2} - \frac{c r_a}{2 r_c} \frac{u^2}{h + \eta} \quad (5)$$

$$\frac{r_c}{r_a} \varepsilon u \frac{\partial v}{\partial s} + v \frac{\partial v}{\partial n} - \frac{n_o}{r_a} u^2 = \frac{1}{F_r^2} \frac{\partial h}{\partial n} \quad (6)$$

where Eq. 3 is the continuity equation, Eq. 4 the sectional discharge and Eqs. 5 & 6 the momentum equations in s and n directions, respectively. Here $c = fR/H$, $\varepsilon = B_o/2R$, $h = h_o/H$, $u = u_o/V_o$, $v = v_o/V_o$, $s = s_o/R$, $n = n_o/n_o$, $F_r = V_o/gH$, $R = 2\pi R/L$, $n_o = B/2$, $R = L/2\pi\theta$, $s_o = H$ is the mean average water depth over one single bend, u_o and v_o = depth-averaged velocity in s and n directions, respectively and l = the slope of the transverse average level of the bed. The main symbols in this paper are illustrated in Fig. 2.

The boundary conditions are nondimensionalized as follows (3):

$$\begin{aligned} v &= 0 & \text{at } n &= \pm 1 \\ u &= u_1(n) & \text{at } s &= s_o \text{ (upstream end)} \\ \frac{1}{2} \int_{-1}^1 h \, dn &= 1 & \text{at } s &= s_d \text{ (downstream end)} \end{aligned} \quad (7)$$

2.2 Solutions by the Perturbation Method

In present analysis the perturbation method is used in terms of ε to solve the governing equations. The perturbed expression for the hydraulic quantities are presented as follows:

$$\begin{aligned} h &= h_o + \varepsilon h_1 + \varepsilon^2 h_2 + \dots \\ u &= u_o + \varepsilon u_1 + \varepsilon^2 u_2 + \dots \\ v &= v_o + \varepsilon v_1 + \varepsilon^2 v_2 + \dots \\ u_1 &= u_{10} + \varepsilon u_{11} + \varepsilon^2 \left(n^2 - \frac{1}{3} \right) u_{12} + \dots \\ \eta &= \eta_o + \varepsilon \eta_1 + \varepsilon^2 \eta_2 + \dots \\ &= \varepsilon n (a_o \sin ks + a_1 \cos ks) + \varepsilon^2 \left(n^2 - \frac{1}{3} \right) (a_2 + a_3 \sin 2ks + a_4 \cos 2ks) \end{aligned} \quad (8)$$

where u_{10} , u_{11} and u_{12} in the fourth equation of Eq. 5 are constants (3). The fifth equation of Eq. 5 is an equation which determines the equilibrium bed profile and it is found to be a quadratic equation with respect to the lateral coordinate, n , in continuous bends, where $\eta = (H_0 - h)/H_0$ and a_0 , a_1 , a_2 , a_3 and a_4 are constants. It is assumed that the flow is in quasi-uniform. The derivation of the solution follows the line described in the preceding paper (3).

2.2.1 Zeroth Order Solutions

The zeroth order solutions from equilibrium bed are the same in case of rectangular channel ($\eta_0 = 0$). The solutions are shown as follows:

$$\begin{aligned} v_0 &= 0 \\ h_0 &= 1 \\ u_0 &= 1 \\ V &= (2gIR/c)^{1/2} \end{aligned} \quad (9)$$

where the fourth relation in Eq. 9 shows the condition of the normal flow.

2.2.2 First Order Solutions

The nondimensional expressions for the first order solution are found out as follows:

$$\begin{aligned} h &= h_0 + \varepsilon h_1 = 1 + \varepsilon n F_r^2 \cos ks \\ u &= u_0 + \varepsilon u_1 = 1 + \varepsilon n (A \sin ks + B \cos ks + C_3 e^{-cs}) \\ v &= v_0 + v_1 = 0 \end{aligned} \quad (10)$$

where

$$\begin{aligned} A &= \frac{kc}{2(k^2 + c^2)} (1 + F_r^2 + a_1) + \frac{a_0 c^2}{2(k^2 + c^2)} \\ B &= \frac{1}{k^2 + c^2} \left[\frac{c^2}{2} (F_r^2 - 1 + a_1) - k^2 - \frac{ck}{2} a_0 \right] \\ C_3 &= (u_{11} - A \sin ks_0 - B \cos ks_0) e^{cs} \end{aligned} \quad (11)$$

2.2.3 Second Order Solutions

The nondimensional expression of the second order solution are obtained as follows:

$$\begin{aligned} h_2(s, n) &= h_{21} + h_{22} \\ h_{21} &= \frac{F_r^2}{2} \left(n^2 - \frac{1}{3} \right) [A \sin 2ks + B_2 \cos 2ks + 1] + 2C_3 e^{-cs} \cos ks \\ h_{22} &= \frac{F_r^2}{2} [J_1 \sin 2ks + J_2 \cos 2ks + J_3 e^{-cs} \sin ks + J_4 e^{-cs} \cos ks \\ &\quad + J_5 e^{-cs} + J_6 + J_7 e^{-cs}] \dots (12) \\ u_2(s, n) &= \frac{ck_1 + 2kk_2}{c^2 + 4k^2} \sin 2ks + \frac{ck_1 - 2kk_2}{c^2 + 4k^2} \cos 2ks + \frac{k_4}{k} e^{-cs} \sin ks \end{aligned}$$

$$\begin{aligned} & \frac{K_3}{k} e^{-cs} \cos ks - \frac{K_5}{c} e^{-cs} + \frac{K_6}{c-C_2} e^{-c_2 s} + \frac{K_7}{c} + (n^2 - \frac{1}{3}) u_{12} e^{c(s_0-s)} \\ & - e^{c(s_0-s)} \left[\frac{K_1 c + 2kK_2}{c^2 + 4k^2} \sin 2ks_0 + \frac{cK_2 - 2kK_1}{c^2 + 4k^2} \cos 2ks_0 + \right. \\ & \left. \frac{K_4}{k} e^{-cs_0} \sin ks_0 - \frac{K_3}{k} e^{-cs_0} \cos ks_0 - \frac{K_5}{c} e^{-2cs_0} + \frac{K_6}{c-C_2} e^{-c_2 s_0} + \frac{K_7}{c} \right] \\ v_2 = & (1-n^2) (D \cos ks + E \sin ks + C_4 e^{-cs}) \end{aligned}$$

where $B_2 = B - 1/2$. $J_1, J_2, J_3, J_4, J_5, J_6, J_7, K_1, K_2, K_3, K_4, K_5, K_6$ and K_7 are constants which we can not show their detailed expression due to the restriction on space. h_{21} in Eq. 12 shows the deviation of the water surface from the sectional average one.

Through Eqs. 9 to 12 we reach the full expressions up to the second order solutions. The shear stress is determined by Eq. 2.

3. COMPARISON OF THE THEORY AND EXPERIMENTAL DATA

3.1 Transverse Distribution of the Depth-Averaged Velocity

The geometry of the flume in our laboratory has been shown in previous paper (4). The coefficient expressing of the idealized bed topography in the fifth equation of Eq. 8 are as follows: $a_0 = 0.673$, $a_1 = 3.110$, $a_2 = 7.357$, $a_3 = 3.708$ and $a_4 = 2.712$. Fig. 3 shows the comparison between the measured and the calculated values of the transverse depth-averaged velocity. The theoretical transverse velocity distribution shows that the highest velocity which appears near the inner bank in the first half of the bend tends to shift towards the outer bank as the flow goes downstream. For our experimental data, unfortunately we don't have measured values near the inner bank at the area between section $\pi/4$ and section $5\pi/12$ due to the shallowness of the water depth. It is seen from Fig. 3 that the theoretical values show a good agreement with the measured values in magnitude as well as the transverse profile. The

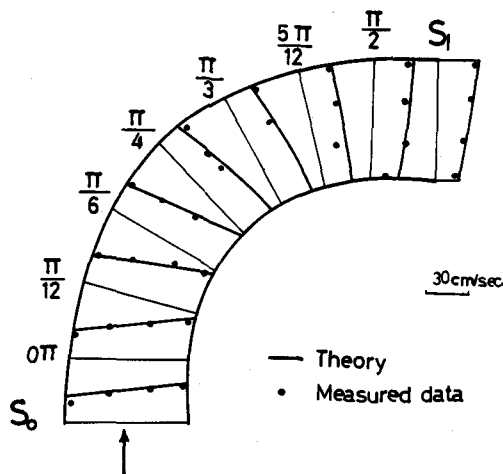


Fig. 3 Distribution of depth-averaged longitudinal velocity (second order)

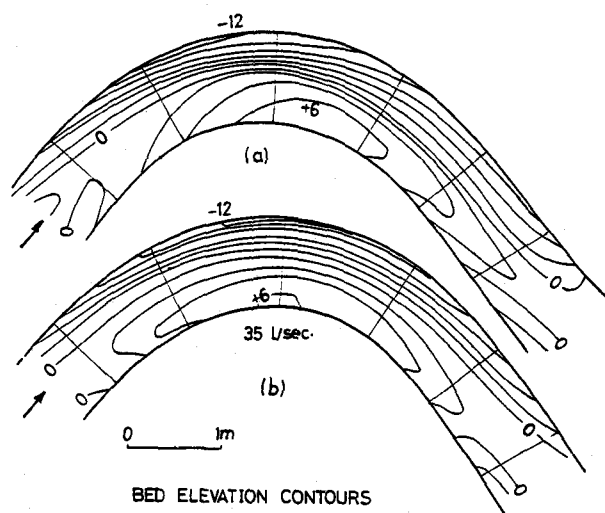


Fig. 4 Bed topography
 (a) Measured by Hooke Run 35
 (b) Simulated by Eq. (8)₅

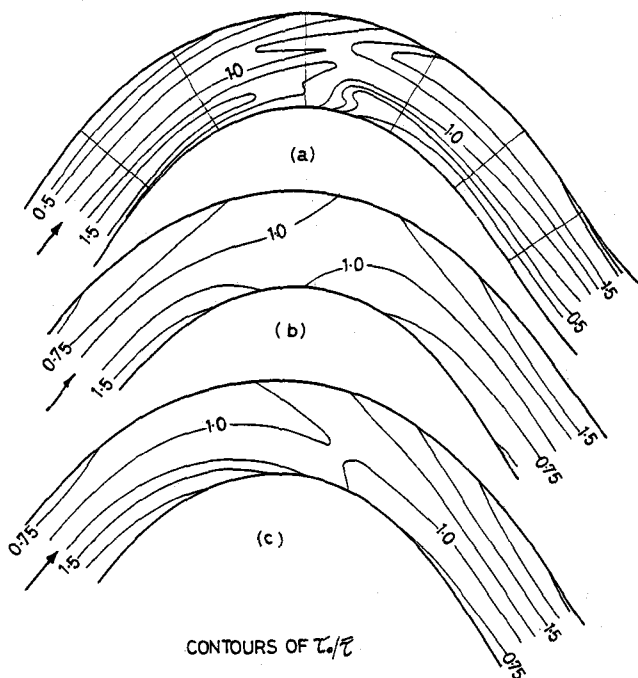


Fig. 5 Shear stress distribution
 (a) Measured by Hooke Run 35
 (b) Calculated (First order)
 (c) Calculated (Second order)

depth-averaged velocity distribution by the first order theory is linear for the transverse direction variation and the magnitude estimated by the first order theory seems satisfactory. The general behavior of the theoretical results is also supported by other experimental data (5). At the point of appearance of the highest transverse velocity, the present theory differs from Engelund's (1) theory which shows that the highest velocity moves towards the outer bank within for the first half of the unit bend.

3.2 Comparison With Hooke's Experiment

The centerline geometry of Hooke's flume coincides with a sine-generated curve (2). Now, to compare the bed shear distribution measured by Hooke and the theoretical values calculated by Eq. 2, it is needed to determine an idealized bed topography in order to calculate the depth-averaged flow. As an example for the comparison, Hooke's run 35 has been considered. Fig. 4 shows the measured and the calculated bed topography. It is found out the constants in the fifth equation of Eq. 8 equal to $a_0 = 0.393$, $a_1 = 4.465$, $a_2 = 8.938$, $a_3 = -0.827$ and $a_4 = 2.013$. The overall agreement is fairly good for the comparison of shear stress.

The results of the first and the second order estimation of the shear stress and the measured one are shown in Fig. 5. It is seen that essential distribution pattern is reproduced by both the first and the second order theory.

4. CONCLUSIONS

1. The theory shows good agreement with the variation of the measured depth-averaged flow velocity and bottom shear stress along meandering channels.

2. The contribution of the second order term in the theory does not seem to be substantial. However, for the detailed discussion more precise measurement is needed.

REFERENCES

- 1) Engelund, F. "Flow and bed topography in channel bends", Proc. ASCE, vol. 100, Hy. 11, pp. 1631- 1647, 1974.
- 2) Hooke, R.L. "shear- stress and sediment distrebuton in meander bend" UNGI-report 30, Univ. of Uppsala, 58 p., 1974.
- 3) Ikeuchi, K and N. Tamai "Evoulution of depth-averaged flow field in meandering channels, Proc. JSCE, No. 334, pp. 89- 101, 1983 (in japanese).
- 4) Tamai, N. and Ali A. Mohamed "Velocity profiles in continuous bends over idealized bars" Annual meeting of JSCE, 1984.
- 5) Yen, C.L. " Bed topography effect on flow in a meander" Proc. ASCE, vol. 96, No. Hy. 1, pp. 57-73, 1970.